

Development of Ethyl Hydrazide-Based Selective Histone Deacetylase 6 (HDAC6) PROTACs

Daniel Stopper^{1§}, Irina Honin^{1§}, Felix Feller¹, Finn K. Hansen^{1}*

¹ Department of Pharmaceutical and Cell Biological Chemistry, Pharmaceutical Institute, University of Bonn, 53121 Bonn, Germany

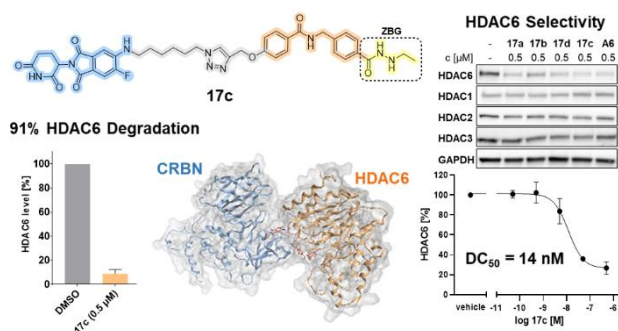
§ These authors contributed equally

* Corresponding author:

Prof. Dr. Finn K. Hansen, Pharmaceutical and Cell Biological Chemistry, Pharmaceutical Institute, University of Bonn, An der Immenburg 4, 53121 Bonn, Germany. Tel.: (+49) 228 73 5213. Fax: (+49) 228 73 7929. E-mail: finn.hansen@uni-bonn.de.

ABSTRACT

Histone deacetylases (HDACs) are promising targets for epigenetic drug discovery. Additionally, targeted degradation of HDACs has emerged as a novel approach in medicinal chemistry and chemical biology. However, most inhibitors and degraders rely on the potentially genotoxic hydroxamate as a zinc-binding group (ZBG). In this study, we present the development of HDAC6-directed proteolysis-targeting chimeras (PROTACs) featuring an ethyl hydrazide moiety as an alternative ZBG. This approach avoids the genotoxicity concerns of hydroxamates while maintaining potent HDAC6 degradation. We synthesized a series of CRBN- and VHL-recruiting PROTACs and identified several potent HDAC6 degraders (HDAC6 D_{max} > 80%). Among these, **17c** was the most effective, achieving an HDAC6 degradation of 91% and a DC_{50} value of 14 nM. Further characterization proved that **17c** acts *via* the ubiquitin-proteasome system and chemoproteomics confirmed selective HDAC6 degradation over other HDAC isoforms.



KEYWORDS

Histone deacetylase (HDAC); HDAC degradation; Proteolysis targeting chimeras (PROTACs); Targeted Protein Degradation (TPD); Zinc-binding group (ZBG)

INTRODUCTION

The posttranslational modification of histone proteins is a key mechanism in epigenetics. This mechanism includes the acetylation, methylation, phosphorylation, and other chemical modifications of the histone proteins.¹ The acetylation is driven by histone acetyl transferases (HATs), while the deacetylation is catalyzed by histone deacetylases (HDACs). The latter has been under continuous investigation for drug discovery and beyond.²

So far, eleven zinc-dependent and seven NAD⁺-dependent HDAC enzymes have been identified, which are categorized in four classes. Class I consists of the isoforms HDAC1, 2, 3, and 8 and is mainly responsible for the cleavage of acetyl groups from histone lysine side chains. Inhibition of this class usually results in cytotoxic effects.³ Class II is further divided into two subclasses. Class IIa encompasses HDAC4, 5, 7, and 9, while class IIb includes HDAC6 and 10. Class III enzymes are the NAD⁺-dependent sirtuins and contain seven isoforms (Sirt1-7). Finally, class IV comprises only one enzyme, which is HDAC11. The FDA approval of four HDAC inhibitors as anticancer drugs (vorinostat, panobinostat, belinostat, and romidepsin) has shown the great potential of HDAC inhibitors in oncology drug development. The recent approval of givinostat for the treatment of *Duchenne* muscular dystrophy (DMD) highlights the expanding applications of HDAC inhibitors beyond oncology.⁴

In recent years, it has become evident that HDACs possess functions besides their traditional role in catalyzing the removal of acetyl or acyl residues.⁵⁻⁷ Consequently, targeted knock-down of these enzymes has the potential to profoundly affect disease-mediated cellular functions that are beyond the scope of traditional inhibition. One way to induce targeted degradation of HDACs is the development of HDAC proteolysis targeting chimeras (PROTACs). PROTACs are heterobifunctional molecules which consist of a ligand that binds to the protein of interest (POI), an E3 ligase ligand, and an appropriate spacer that connects the two binders. Through simultaneous binding to the E3 ligase and the POI proximity is induced and the E3 ligase is recruited to polyubiquitinylate the target which leads to its proteasomal degradation.⁸ In recent years, hydrazides have emerged as possible zinc-binding groups for HDAC inhibitors and degraders.⁹ Especially *N*-substituted hydrazides have gained attention in HDAC inhibitor and PROTAC development. Longer chain alkyl hydrazides have been shown to

potently inhibit and degrade HDAC8,^{10–12} whereas *n*-propyl hydrazides have emerged as a class I selective zinc-binding group (ZBG).^{13,14} Ethyl hydrazides have also appeared and were shown to be a non-selective ZBG.¹⁵ But with fine-tuning of the cap group, this ZBG can also be employed to develop selective HDAC6 inhibitors.¹⁶

In this study, we aimed to develop HDAC6 degraders utilizing an ethyl hydrazide ZBG, as no published reports on ethyl hydrazide-based HDAC6 PROTACs are currently available.

RESULTS AND DISCUSSION

Design and synthesis. The bifunctional molecules were designed in a systematic manner (Figure 1). The HDAC binding ligand was derived from our previously developed degrader molecule **A6**,¹⁷ except that the linker in the HDAC inhibitor pharmacophore was changed to a benzyl moiety to achieve better HDAC6 selectivity.¹⁸ The ZBG within the HDAC6 ligand was changed from a hydroxamate to an ethyl hydrazide group. To attach the HDAC6 ligand to the spacer of the final PROTACs, we chose two distinct connecting units. One is a carboxamide directly connected to the phenyl ring of the HDAC6 ligand and the other is the bioisosteric 1,2,3-triazole ring,¹⁹ which is attached to the HDAC6 ligand by an ether group. The linkers were derived from **A6** as well, and thus a C8 alkyl linker was chosen for the compounds bearing the carboxamide as a connecting unit, while C6 alkyl linkers were selected for the triazole-containing compounds. This was done in order to achieve a similar total distance between the E3 ligase ligand and the HDAC6 ligand. To compare alkyl versus polyethylene glycol (PEG) linkers, we also included PEG2 for carboxamides and PEG1 for triazole-based PROTACs. To investigate the effect of different E3 ligases we chose two different E3 recruiters. Firstly, we selected a CRL4^{CRBN} engaging ligand like in **A6** but changed it from the classical thalidomide to a 6-fluorothalidomide, which is connected in 5-position to the PROTAC spacer by an amine bond. Secondly, we used the CRL2^{VHL} binding ligand **VH032**-amine, which is connected to the spacer by an amide group.²⁰

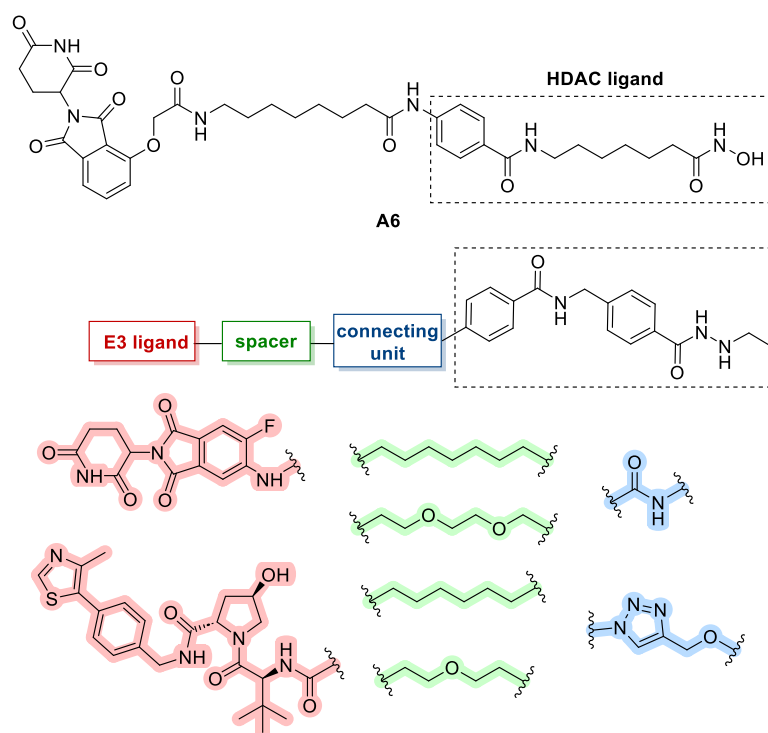
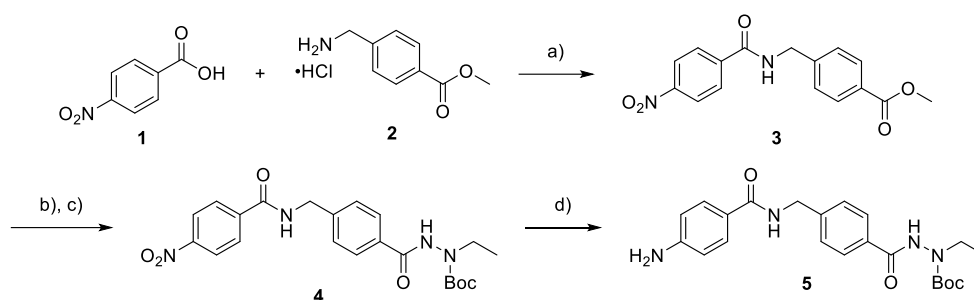


Figure 1. Design of ethyl hydrazide-based PROTACs derived from our previously developed HDAC6 degrader **A6**.¹⁷

The synthesis of the HDAC ligand was done using two different pathways, one for the synthesis of the amide-connected ligands and the other for the triazole connected compounds. The aromatic amine **5** was synthesized for the use in amide-connected PROTACs (Scheme 1). An amide coupling using TBTU as a coupling agent generated intermediate **3**. The methyl ester was then saponified by aqueous NaOH in a THF/MeOH mixture. Subsequently, 1-Boc-1-ethylhydrazine was introduced by another coupling reaction using HATU as the coupling agent. Finally, the nitro group of **4** was reduced by catalytic hydration in MeOH with a palladium catalyst to afford the key intermediate **5**.

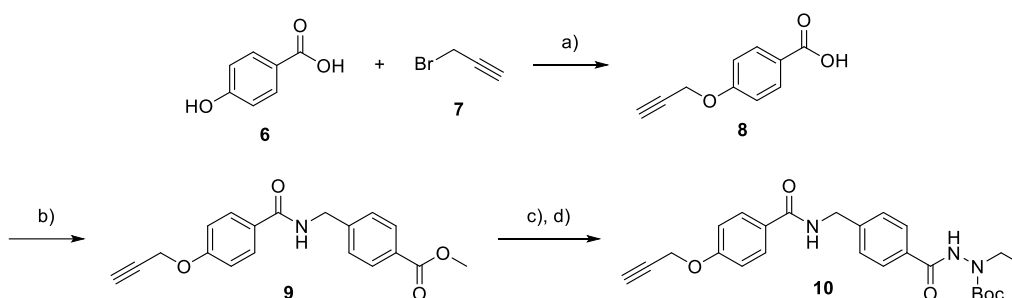
Scheme 1. Synthesis of the aromatic amine key intermediate **5**.^a



^aReagents and conditions: a) TBTU, DIPEA, DMF, rt, overnight. b) NaOH aq., THF/MeOH (5/2 (v/v)), rt, overnight. c) HATU, 1-Boc-1-ethylhydrazine, DIPEA, DMF, rt, overnight. d) Pd/C, H₂, MeOH, rt, 2 h.

The terminal propargyl ether **10** was synthesized for the desired 1,2,3-triazole connected compounds (Scheme 2). Here, we synthesized ether **8** by Williamson ether synthesis of 4-hydroxybenzoic acid (**6**) and propargyl bromide (**7**) using potassium carbonate as a base. The carboxylic acid (**8**) was then subjected to an amide coupling using HATU in DMF and methyl 4-(aminomethyl) benzoate. Again, the resulting methyl ester (**9**) was hydrolyzed and coupled with 1-Boc-1-ethylhydrazine using HATU to obtain the key intermediate **10**.

Scheme 2. Synthesis of the propargyl ether key intermediate **10**.^a

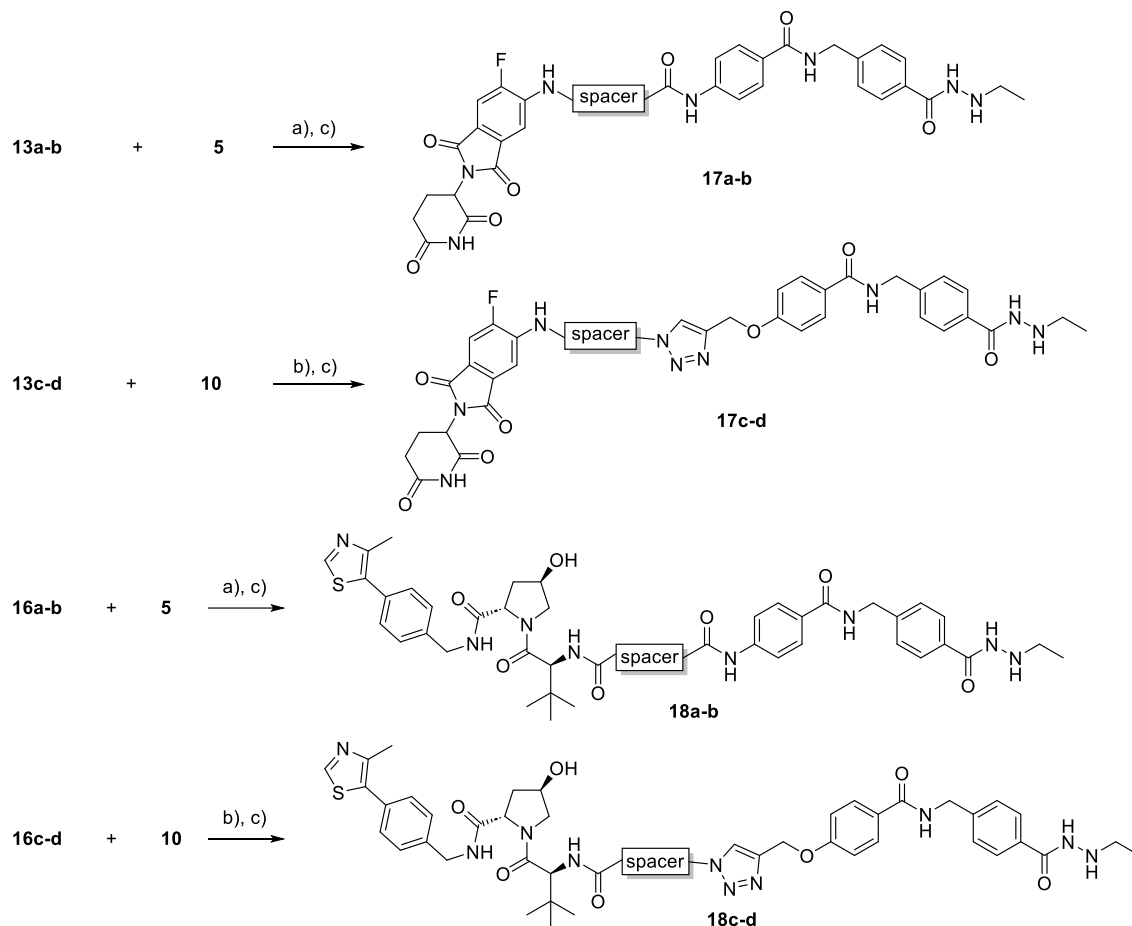


^aReagents and conditions: a) K₂CO₃, DMF, H₂O, rt, overnight. b) Methyl 4-(aminomethyl) benzoate, HATU, DIPEA, DMF, rt, overnight. c) NaOH aq., THF/MeOH (5/2 (v/v)), rt, overnight. d) HATU, 1-Boc-1-ethylhydrazine, DIPEA, DMF, rt, overnight.

To connect the spacers with the CRL4^{CRBN} engaging building block, 5,6-difluorothalidomide **11** was substituted by nucleophilic aromatic substitution (S_NAr) in DMSO at 110 °C using the respective spacers **12a-d** as the amine nucleophiles (Scheme 3). For the synthesis of the *von Hippel-Lindau* (VHL)-based PROTACs, **14** (VH032-amine) was coupled to the respective spacers **15a-d** as carboxylic acids by amide coupling. For the synthesis of the intermediates **16a,b** a method described in patent literature²¹

deprotection of the hydrazide moiety using trifluoroacetic acid (TFA) to form the cereblon-recruiting degraders **17a-d** and the VHL-recruiting PROTACs **18a-d** (Scheme 5).

Scheme 5. Synthesis of PROTACs **17a-d** and **18a-d**.^a



^aReagents and conditions: a) PyBrOP, DIPEA, DMF, rt, overnight. b) CuSO₄×5H₂O, L-ascorbic acid, TBTA, THF, H₂O, DMF, rt, overnight. c) TFA, DCM, rt, 2-24 h.

***In vitro* HDAC inhibition assays.** The *in vitro* inhibition of HDAC enzymes was conducted to investigate the inhibitory potency and the isoform selectivity of the synthesized PROTACs **17a-d** and **18a-d**. Vorinostat (SAHA) and **A6** were included as control compounds. In detail, the inhibition of the nuclear class I isoforms HDAC1-3 and the cytoplasmic class IIb isoform HDAC6 was evaluated. The results are depicted in Table 1. All compounds showed low single-digit micromolar inhibitory activity against HDAC1 and HDAC2, with the exception of **17a,b**, which demonstrated high submicromolar inhibitory activity against these two isoforms, and **17d**, which inhibited HDAC2 with a slightly submicromolar half maximal inhibitory concentration (IC₅₀) value. All compounds showed

submicromolar inhibition of HDAC3, making all tested compounds preferable HDAC3 inhibitors over HDAC1 and 2. **18a** exhibited the lowest IC₅₀ value of 0.126 μM against HDAC3. The class IIb isoform HDAC6, was preferably inhibited by all compounds except for **18a**, which showed the highest activity against HDAC3. All other compounds inhibited HDAC6 with IC₅₀ values ranging from 0.108 to 0.594 μM. These assays confirmed target inhibition and, consequently, binding. Although most compounds showed a preference for HDAC6 inhibition, the nuclear isoforms HDAC1-3 were also inhibited.

Table 1. Inhibition of HDAC1-3 and HDAC6.

Cmpd	E3 Ligase	Linker	Connecting Unit	HDAC1 IC₅₀ [μM]^[a,b]	HDAC2 IC₅₀ [μM]^[a,b]	HDAC3 IC₅₀ [μM]^[a,b]	HDAC6 IC₅₀ [μM]^[a]
17a	CRBN	C8	Amide	0.749 ± 0.085	0.727 ± 0.092	0.238 ± 0.017	0.108 ± 0.009
17b	CRBN	PEG2	Amide	0.879 ± 0.091	0.848 ± 0.048	0.378 ± 0.034	0.238 ± 0.020
17c	CRBN	C6	Triazole	2.20 ± 0.25	2.37 ± 0.12	0.611 ± 0.061	0.295 ± 0.009
17d	CRBN	PEG1	Triazole	1.27 ± 0.22	0.975 ± 0.001	0.332 ± 0.016	0.224 ± 0.013
18a	VHL	C8	Amide	1.44 ± 0.01	1.45 ± 0.22	0.126 ± 0.028	0.234 ± 0.059
18b	VHL	PEG2	Amide	3.41 ± 0.52	3.25 ± 0.68	0.729 ± 0.196	0.594 ± 0.057
18c	VHL	C6	Triazole	2.31 ± 0.30	2.86 ± 0.19	0.417 ± 0.029	0.164 ± 0.041
18d	VHL	PEG1	Triazole	1.66 ± 0.41	1.54 ± 0.029	0.244 ± 0.049	0.215 ± 0.047
NC-17c	-	C6	Triazole	2.34 ± 0.31	2.05 ± 0.81	0.537 ± 0.012	0.389 ± 0.019
A6	-	-	-	0.136 ± 0.004	0.276 ± 0.069	0.164 ± 0.006	0.007 ± 0.001
SAHA	-	-	-	0.121 ± 0.012	0.217 ± 0.037	0.101 ± 0.010	0.036 ± 0.0004

^[a] mean ± SD, results from two individual experiments. ^[b] 1 h preincubation of enzyme and inhibitor at rt.

Influence of 17a-d and 18a-d on cell viability. To evaluate the cytotoxicity of the synthesized PROTACs, all compounds were initially tested for their antiproliferative activity against the multiple myeloma cell line MM.1S by a CellTiter-Glo™ viability assay. The results are summarized in Table 2. Most compounds showed no significant cytotoxicity in the concentration range of the assay. Only **17a** and **17c**, both fluorothalidomide-based PROTACs, showed a moderate toxicity with IC₅₀ values of 18.4 and 24.9 μM, respectively. Since HDAC6-selective inhibitors usually also demonstrate minimal toxicity²² and inhibition of other HDAC isoforms was determined to be lower, the results align with our expectations from the HDAC inhibition assays.

Table 2. Effect of synthesized PROTACs on the viability of the multiple myeloma MM1.S cells.

Compound	E3 Ligase	Linker	Connecting Unit	IC ₅₀ [μM] ^[a]
17a	CRBN	C8	Amide	18.4 ± 1.6
17b	CRBN	PEG2	Amide	>50.0 ^[b]
17c	CRBN	C6	Triazole	>50.0 ^[b]
17d	CRBN	PEG1	Triazole	24.9 ± 4.4
18a	VHL	C8	Amide	>50.0 ^[b]
18b	VHL	PEG2	Amide	>50.0 ^[b]
18c	VHL	C6	Triazole	>50.0 ^[b]
18d	VHL	PEG1	Triazole	>50.0 ^[b]
NC-17c	-	C6	Triazole	>50.0 ^[b]
A6	-	C6	Triazole	>50.0 ^[b]
SAHA	-	-	-	0.800 ± 0.067

^[a] mean ± SD, results from three individual experiments. ^[b] > 50% viability at 50 μM.

Characterization of HDAC6 degradation and selectivity. To assess the HDAC-degrading capabilities of **17a-d** and **18a-d**, we treated multiple myeloma cells (MM.1S) with our test compounds with concentration of 0.5 μM and 5 μM. Compound **A6**, a selective HDAC6 degrader identified in our previous study, was included as a control.¹⁷ MM1.S cells were treated for 24 hours before HDAC6 levels

were determined by immunoblot analysis, as depicted in Table 3 and Figure 2A (Supporting Information). Interestingly, significant HDAC6 degradation was shown by all of the CRBN-engaging compounds **17a-d**, but no degradation of HDAC6 was exhibited by VHL-based compounds **18a-d**. The most potent degradation of 91% was achieved by **17c** at 0.5 μ M. Additionally, **17a-c** showed increased levels of HDAC6 at 5 μ M compared to the levels at 0.5 μ M. This effect was not observed for **17d**. Here, at 5 μ M the HDAC6 degradation was higher (90%) than at 0.5 μ M (85%). It was also investigated whether HDAC1-3 could be degraded by the compounds. As shown in Figure 2B, no degradation of HDAC1-3 was observed for any compound.

Table 3. Degradation of HDAC6 in MM1.S cells at a concentration of 0.5 μ M in MM.1S cells after 24 hours.

Compound	E3 Ligase	Linker	Connecting Unit	HDAC6 Degradation [%] ^[a]
17a	CRBN	C8	Amide	86 \pm 4
17b	CRBN	PEG2	Amide	75 \pm 3
17c	CRBN	C6	Triazole	91 \pm 3
17d	CRBN	PEG1	Triazole	85 \pm 1
18a	VHL	C8	Amide	no degradation
18b	VHL	PEG2	Amide	no degradation
18c	VHL	C6	Triazole	no degradation
18d	VHL	PEG1	Triazole	no degradation
A6	-	-	-	94 \pm 5

^[a] mean \pm SD, results from at least three individual experiments.

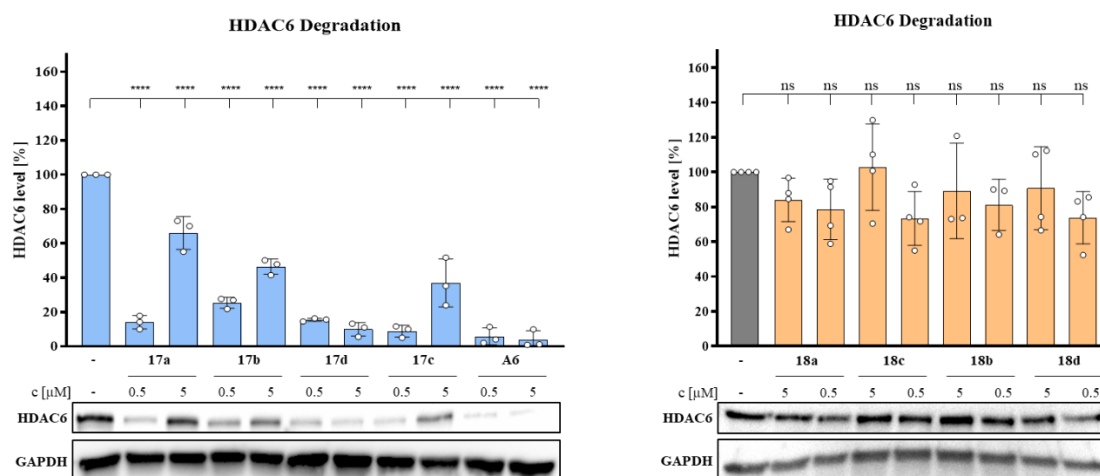
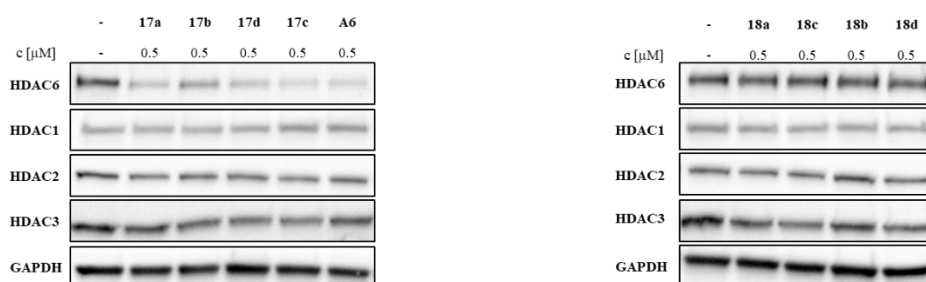
A**B**

Figure 2. Immunoblot analysis of MM.1S cell lysates. **A)** Degradation of HDAC6. Cells were treated with 0.5 or 5 μM of the respective test compound or vehicle (DMSO) for 24 hours. **B)** Evaluation of HDAC6 and HDAC1-3 degradation. Cells were treated with 0.5 μM of test compound or vehicle (DMSO) and otherwise identically treated to A). Representative images from a total of at least three replicates. Significance: ns = $p \geq 0.05$; **** = $p \leq 0.0001$.

Concentration-dependent degradation of HDAC6 by 17c. Next, the degradation efficiency of **17c** was quantified by the determination of a half-maximal degradation concentration (DC_{50}) value *via* automated capillary western blot utilizing the Simple Western™ immunoassay technology (Figure 3). For **17c** a DC_{50} value of 14 nM was determined in MM.1S cells. Overall, our data confirms that **17c** is a highly potent, selective, and non-toxic HDAC6 degrader. Thus, this promising tool compound was selected for a more comprehensive evaluation.

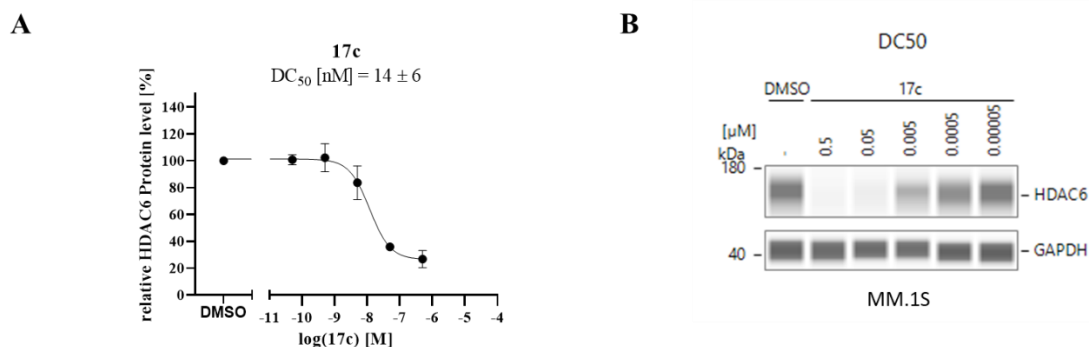


Figure 3. Quantitative Simple Western™ immunoassays show dose-dependent degradation of HDAC6. MM.1S cells were treated with the indicated concentrations of compound **17c** or vehicle (0.5% DMSO) for 24 hours. GAPDH was used as a loading control. **A**) A normalized dose-response curve is shown, with HDAC6 levels in vehicle treated cells set to 100%. The DC_{50} value was determined by nonlinear regression ($\log(\text{inhibitor})$ vs response, three-parameter analysis). Data represents the mean \pm SD of three individual experiments. **B**) Images of a representative simple Western immunoassays.

HDAC6 degradation is dependent on the cyclic imide degron of 17c. To investigate, if the degradation of HDAC6 is mediated by the fluorothalidomide cyclic imide degron of **17c**, a methylated, non-degrading control, **NC-17c** (Figure 4A), was synthesized (see Scheme S1, Supporting Information) and evaluated head-to-head with **17c**. As depicted in Figure 4B, **17c** showed potent degradation of HDAC6, but not of HDAC1. **NC-17c** did not show any degradation of HDAC1 or HDAC6. These results confirm the necessity of the free imide group for HDAC6 degradation, which is essential for binding and recruiting CRBN. Additionally, the hyperacetylation of the HDAC6 substrate α -tubulin was determined by immunoblot analysis (Figure 4B). Notably, hyperacetylation of the substrate was not found in **NC-17c**-treated cells. **NC-17c** was determined to inhibit HDAC6 at $0.389 \mu\text{M}$, which is similar to the inhibitory activity of **17c** ($0.295 \mu\text{M}$, Table 1). Only by degradation of HDAC6 through **17c**, we

found significantly hyperacetylated α -tubulin. This effect was more pronounced at 5 μ M than at 0.5 μ M, which is possibly due to a combination of HDAC6 degradation and inhibition of residual protein.

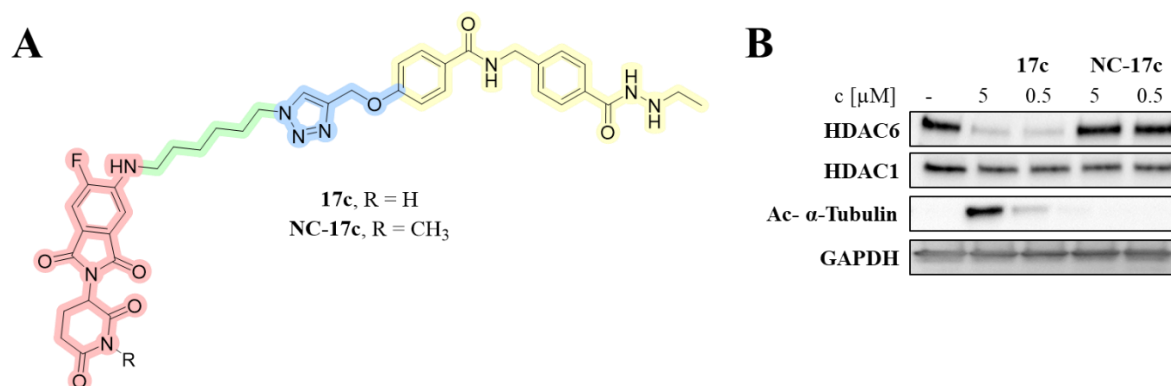


Figure 4. A) Structures of the ethyl-based PROTAC **17c** and the methylated non-degrading control **NC-17c**. B) Immunoblot analysis of HDAC1, HDAC6, and acetylated α -tubulin. MM.1S cells were treated with the compounds **17c** and **NC-17c** for 24 h at 5 μ M and 0.5 μ M. GAPDH was used as a loading control. A representative immunoblot of two individual experiments is shown.

HDAC6 degradation is mediated by the ubiquitin-proteasome system. Proteasomal rescue experiments were performed to confirm that HDAC6 degradation by **17c** is mediated *via* the ubiquitin-proteasome pathway. For this purpose, MM1.S cells were pretreated for 30 minutes with 10 μ M of the binding competitors tubastatin A, pomalidomide or the NEDD8-activating enzyme inhibitor MLN4924 before **17c** was added. As illustrated in Figure 5, HDAC6 levels were almost completely rescued when the cells were pretreated with these compounds. The rescue experiments confirmed that **17c** induced HDAC6 degradation is neddylation dependent and requires the interaction with both CRBN and HDAC6.

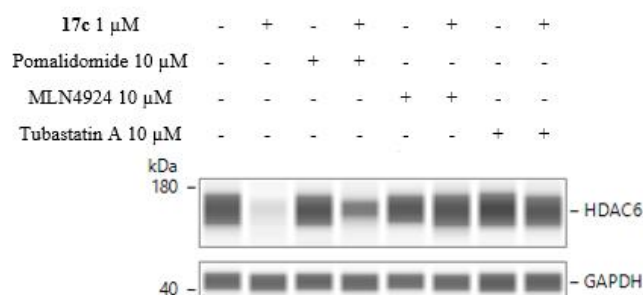


Figure 5. Rescue experiments with **17c** *via* Simple Western™ immunoblot analysis. MM.1S cells were

treated with tubastatin A (10 μ M), pomalidomide (10 μ M), MLN4924 (10 μ M) alone or in combination with **17c** (1 μ M) for 24 h according to the depicted scheme. For co-treatments binding-inhibitors and neddylation inhibitor MLN4924 were added 30 minutes before **17c**. GAPDH was used as loading control. Representative images from a total of n = 3 replicates.

Quantitative chemoproteomic investigation. To investigate the effects of **17c** on the global proteome, a chemoproteomic investigation by quantitative diaPASEF-based mass spectrometry²³ in MM.1S cells was conducted. In total, 5738 proteins were identified and among them, seven Zn²⁺-dependent HDAC isoforms were found. The volcano plot in Figure 6A shows that HDAC6 was significantly reduced in **17c**-treated cells compared to vehicle-treated cells. Additionally, degradation of IKZF3, a CRBN neosubstrate,²⁴ as well as collateral degradation of MIER1, a part of an HDAC1/2 multienzyme complex,²⁵ was observed upon **17c** treatment. The degradation of MIER1 has also been observed in previous chemoproteomic investigations of a HDAC-focused degrader library.²⁶ The degradation of other HDAC isoforms was not observed (Figure 6B). Thus, the HDAC6-selective degradation over other HDAC isoforms, as shown by immunoblotting, could be confirmed.

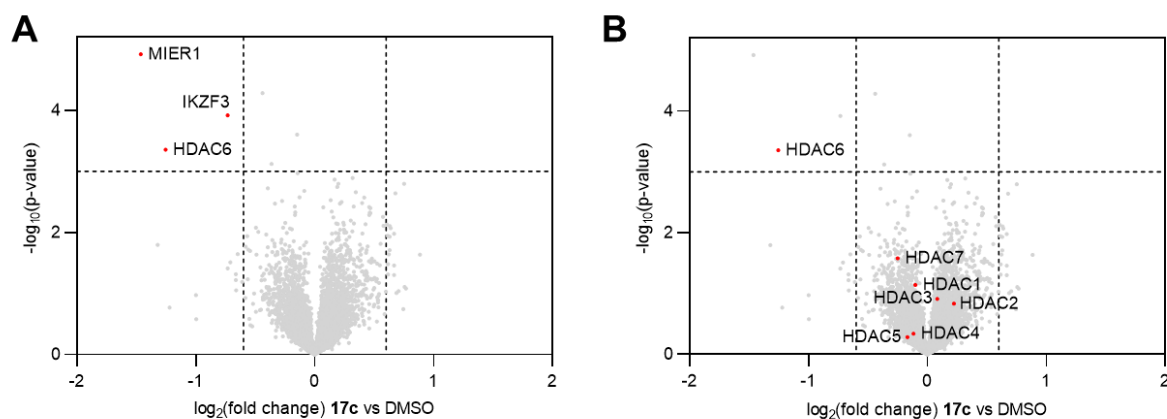


Figure 6. Quantitative diaPASEF-based proteomics for **17c**. MM.1S cells were treated with compound **17c** at 0.5 μ M for 6 h. **A)** Proteins that are significantly degraded are marked red. **B)** All detected HDAC isoforms are marked red. Significant changes comparing the relative protein abundance of treatment to DMSO control comparisons were assessed by moderated t-test as implemented in the limma package within the R framework. The identified proteins were plotted as \log_2 fold change (**17c**/DMSO) vs $-\log_{10}$ of the p -value. Proteins with $-\log_{10}(p\text{-value}) > 3$ ($p\text{-value} < 0.001$) and \log_2 fold change > 0.6 or < -0.6 (translating to 1.5-fold up- or down-regulation) were considered to have significantly changed in abundance. Data are the mean of biological duplicates.

CONCLUSION

In conclusion, our study successfully showcased the synthesis and biological evaluation of novel selective HDAC6-targeting PROTACs with an ethyl hydrazide ZBG. We developed a series of HDAC6 PROTACs by linking a simplified HDAC ligand derived from **A6**,¹⁷ with changes in the linker and ZBG, to either 5-fluorothalidomide or **VH032** *via* different linkers. Among these eight PROTACs, the CRBN-engaging molecules **17a-d** induced selective degradation of HDAC6, while other isoforms were not degraded. The **VH032**-based PROTACs did not induce degradation of any of the analyzed isoforms, although binding to HDAC1-3 and HDAC6 was confirmed through enzyme inhibition assays. The lack of degradation might be due to insufficient ternary complex formation which is crucial for the degradation of the POI. Compound **17c** triggered strong HDAC6 degradation in MM.1S cells (91% at 0.5 μ M), with a DC₅₀ of 14 nM for HDAC6. Notably, **17c** selectively degrades HDAC6 without affecting other HDAC isoforms, as confirmed by immunoblot analysis and quantitative proteomics. An *N*-methylated non-degrading negative control, **NC-17c**, was synthesized and tested head-to-head with **17c** for HDAC1 and HDAC6 degradation and α -tubulin hyperacetylation. It could be shown that in contrast to **17c**, **NC-17c** neither affected HDAC6 levels nor induced hyperacetylation of α -tubulin. To confirm that HDAC6 degradation is mediated by the ubiquitin-proteasome system (UPS) we tested **17c** with different pre-treatments on MM.1S cells. First, **17c** was combined with the CRBN ligand pomalidomide, which resulted in elevated HDAC6 levels compared to **17c** treatment alone. This effect arises from the competitive binding of **17c** and pomalidomide to the CRBN IMiD binding site, resulting in reduced binding of **17c** to this site. Next, the neddylation inhibitor MLN4924 was added to prevent neddylation-dependent proteasomal degradation. The addition of MLN4924 showed a strong rescue of HDAC6 levels indicating that **17c** acts *via* the UPS. Tubastatin A, a selective class IIb HDAC inhibitor, was also added and prevented **17c** from binding to HDAC6, thereby inhibiting ternary complex formation. HDAC6 levels were again rescued by the addition of tubastatin A.

Although **17c** is an unselective HDAC inhibitor, its selective degradation of HDAC6 is rather unexpected. In previous studies, we and other groups found selective degradation of HDAC6 mediated by CRBN-recruiting non-selective HDAC ligand-containing PROTACs.^{17,27} **17c** represents such a degrader, since HDAC assays showed a non-selective HDAC inhibition profile similar to that of **A6**.

Furthermore, proteomic analysis confirmed selective reduction of HDAC6 levels as well as collateral degradation of MIER1 by **17c**. A possible mechanism for degradation of MIER1, could be that **17c** forms a ternary complex with the HDAC1/2-MIER1 complex and the CRL4^{CRBN} E3 ligase, leading to the specific (poly)ubiquitination of MIER1 but not of HDAC1/2 and thus to MIER1 degradation. This mechanism was also discussed by Xiong, Donovan *et al.* in their chemo-proteomics exploration of HDAC degradability.²⁶

To conclude, our findings provide valuable insights into the development of new selective HDAC6 degraders based on an alternative ZBG, which hold promise for therapeutic application in HDAC6 related diseases. Furthermore, our compounds resemble the first reported hydrazide-based selective HDAC6-targeting PROTACs.

ACKNOWLEDGEMENTS

We thank Katherine A. Donovan, Eric S. Fischer and the Fischer Lab Degradation Proteomics Initiative for collection of the global proteomics data supported by NIH CA214608 and CA218278.

Funding Sources

The work of I.H. and F.K.H. is funded by the Deutsche Forschungsgemeinschaft (DFG, German Research Foundation) – GRK2873 (494832089). D.S. and F.K.H. acknowledge financial support by the Deutsche Forschungsgemeinschaft (DFG) (HA 7783/1-2). The new NMR console for the 500 MHz NMR spectrometer used in this research was funded by the Deutsche Forschungsgemeinschaft (DFG, German Research Foundation) under project number 507275896.

DATA DEPOSITION

Global proteomics data will be publicly available at the Fischer Lab's Proteomics database: <https://proteomics.fischerlab.org>

ABBREVIATIONS

Cmpd	Compound
CRBN	Cereblon
CRL4	Cullin-RING-ubiquitin (E3) ligase complex
DC ₅₀	Half-maximal degradation concentration
DCM	Dichloromethane
diaPASEF	Data-independent acquisition of parallel accumulation-serial fragmentation
DIPEA	<i>N,N</i> -Diisopropylethylamine
D _{max}	Maximal degradation
DMD	<i>Duchenne</i> muscular dystrophy
DMF	<i>N,N</i> -Dimethylformamide
DMSO	Dimethylsulfoxide
DNA	Deoxyribonucleic acid
EDC	1-Ethyl-3-(3-dimethylaminopropyl)carbodiimide
GAPDH	Glyceraldehyde 3-phosphate dehydrogenase
HAT	Histone acetyl transferase
HATU	1-[Bis(dimethylamino)methylene]-1 <i>H</i> -1,2,3-triazolo[4,5- <i>b</i>]pyridinium-3-oxide hexafluorophosphate
HDAC	Histon deacetylase
HOAt	1-Hydroxy-7-azabenzotriazole
HPLC	High-performance liquid chromatography
IC ₅₀	Half maximal inhibitory concentration
IKZF3	IKAROS Family Zinc Finger 3
IMiD	Immunomodulatory imide drugs
MeOH	Methanol
MIER1	Mesoderm induction early response protein 1
MM.1S	Multiple myeloma steroid sensitive cell line
NAD ⁺	Nicotinamide adenine dinucleotide
NaOH	Sodium hydroxide
PEG	Polyethylene glycol
POI	Protein of interest
PROTAC	Proteolysis targeting chimera
PyBrOP	Bromotripyrrolidinophosphonium hexafluorophosphate
rt	Room temperature
SAHA	Suberoylanilide hydroxamic acid
SD	Standard deviation
S _N Ar	Nucleophilic aromatic substitution
TBTA	Tris[(1-benzyl-1 <i>H</i> -1,2,3-triazol-4-yl)methyl]amine
TBTU	2-(1 <i>H</i> -Benzotriazole-1-yl)-1,1,3,3-tetramethyluronium tetrafluoroborate
TFA	Trifluoroacetic acid
THF	Tetrahydrofuran
TPD	Targeted protein degradation
UPS	Ubiquitin-proteasome system

REFERENCES

- (1) Allis, C. D.; Jenuwein, T. The molecular hallmarks of epigenetic control. *Nat. Rev. Genet.* **2016**, *17* (8), 487–500. DOI: 10.1038/nrg.2016.59. 27.06.2016.
- (2) Ho, T. C. S.; Chan, A. H. Y.; Ganesan, A. Thirty Years of HDAC Inhibitors: 2020 Insight and Hindsight. *J. Med. Chem.* **2020**, *63* (21), 12460–12484. DOI: 10.1021/acs.jmedchem.0c00830. 16.07.2020.
- (3) Abdallah, D. I.; Araujo, E. D. de; Patel, N. H.; Hasan, L. S.; Moriggl, R.; Krämer, O. H.; Gunning, P. T. Medicinal chemistry advances in targeting class I histone deacetylases. *Explor. Target Antitumor Ther.* **2023**, *4* (4), 757–779. DOI: 10.37349/etat.2023.00166. 31.08.2023.
- (4) Mullard, A. FDA approves an HDAC inhibitor for Duchenne muscular dystrophy. *Nat. Rev. Drug Discov.* **2024**, *23* (5), 329. DOI: 10.1038/d41573-024-00066-8.
- (5) Harding, R. J.; Franzoni, I.; Mann, M. K.; Szweczyk, M. M.; Mirabi, B.; Ferreira de Freitas, R.; Owens, D. D. G.; Ackloo, S.; Scheremetjew, A.; Juarez-Ornelas, K. A.; Sanichar, R.; Baker, R. J.; Dank, C.; Brown, P. J.; Barsyte-Lovejoy, D.; Santhakumar, V.; Schapira, M.; Lautens, M.; Arrowsmith, C. H. Discovery and Characterization of a Chemical Probe Targeting the Zinc-Finger Ubiquitin-Binding Domain of HDAC6. *J. Med. Chem.* **2023**, *66* (15), 10273–10288. DOI: 10.1021/acs.jmedchem.3c00314. 27.07.2023.
- (6) Magupalli, V. G.; Negro, R.; Tian, Y.; Hauenstein, A. V.; Di Caprio, G.; Skillern, W.; Deng, Q.; Orning, P.; Alam, H. B.; Maliga, Z.; Sharif, H.; Hu, J. J.; Evavold, C. L.; Kagan, J. C.; Schmidt, F. I.; Fitzgerald, K. A.; Kirchhausen, T.; Li, Y.; Wu, H. HDAC6 mediates an aggressive-like mechanism for NLRP3 and pyrin inflammasome activation. *Science* **2020**, *369* (6510). DOI: 10.1126/science.aas8995.
- (7) Nguyen, H. C. B.; Adlanmerini, M.; Hauck, A. K.; Lazar, M. A. Dichotomous engagement of HDAC3 activity governs inflammatory responses. *Nature* **2020**, *584* (7820), 286–290. DOI: 10.1038/s41586-020-2576-2. 05.08.2020.
- (8) Tsai, J. M.; Nowak, R. P.; Ebert, B. L.; Fischer, E. S. Targeted protein degradation: from mechanisms to clinic. *Nat. Rev. Mol. Cell Biol.* **2024**. DOI: 10.1038/s41580-024-00729-9. 29.04.2024.
- (9) Carreiras, M. d. C.; Marco-Contelles, J. Hydrazides as Inhibitors of Histone Deacetylases. *J Med Chem* **2024**. DOI: 10.1021/acs.jmedchem.4c00541. 02.08.2024.
- (10) Sun, P.; Wang, J.; Khan, K. S.; Yang, W.; Ng, B. W.-L.; Ilment, N.; Zessin, M.; Bülbül, E. F.; Robaa, D.; Erdmann, F.; Schmidt, M.; Romier, C.; Schutkowski, M.; Cheng, A. S.-L.; Sippl, W. Development of Alkylated Hydrazides as Highly Potent and Selective Class I Histone Deacetylase Inhibitors with T cell Modulatory Properties. *J. Med. Chem.* **2022**, *65* (24), 16313–16337. DOI: 10.1021/acs.jmedchem.2c01132. 30.11.2022.
- (11) Xiao, Y.; Awasthee, N.; Liu, Y.; Meng, C.; He, M. Y.; Hale, S.; Karki, R.; Lin, Z.; Mosterio, M.; Garcia, B. A.; Kridel, R.; Liao, D.; Zheng, G. Discovery of a Highly Potent and Selective HDAC8 Degradator: Advancing the Functional Understanding and Therapeutic Potential of HDAC8. *J. Med. Chem.* **2024**. DOI: 10.1021/acs.jmedchem.4c00761. 01.07.2024.
- (12) Zhao, C.; Zhang, J.; Zhou, H.; Setroikromo, R.; Poelarends, G. J.; Dekker, F. J. Exploration of Hydrazide-Based HDAC8 PROTACs for the Treatment of Hematological Malignancies and Solid Tumors. *J. Med. Chem.* **2024**. DOI: 10.1021/acs.jmedchem.4c00836. 01.08.2024.
- (13) Kraft, F. B.; Biermann, L.; Schäker-Hübner, L.; Hanl, M.; Hamacher, A.; Kassack, M. U.; Hansen, F. K. Hydrazide-Based Class I Selective HDAC Inhibitors Completely Reverse Chemoresistance Synergistically in Platinum-Resistant Solid Cancer Cells. *J. Med. Chem.* **2024**, *67* (19), 17796–17819. DOI: 10.1021/acs.jmedchem.4c01817.
- (14) Zhao, C.; Chen, S.; Chen, D.; Río-Bergé, C.; Zhang, J.; van der Wouden, P. E.; Daemen, T.; Dekker, F. J. Histone Deacetylase 3-Directed PROTACs Have Anti-inflammatory Potential by Blocking Polarization of M0-like into M1-like Macrophages. *Angew. Chem. Int. Ed. Engl.* **2023**, *62* (42), e202310059. DOI: 10.1002/anie.202310059. 08.09.2023.
- (15) Stopper, D.; Biermann, L.; Watson, P.; Li, j.; König, B.; Gaynes, M.; Carvalho, L. P. de; Hanl, M.; Hamacher, A.; Schäker-Hübner, L.; Held, J.; Christianson, D.; Kassack, M.; Hansen, F. K. Exploring Alternative Zinc-Binding Groups in Histone Deacetylase (HDAC) Inhibitors Uncovers DS-103 as a Potent Ethylhydrazide-Based HDAC Inhibitor with Chemosensitizing Properties. *ChemRxiv* **2024**. DOI: 10.26434/chemrxiv-2024-837bd.

- (16) Yue, K.; Sun, S.; Jia, G.; Qin, M.; Hou, X.; Chou, C. J.; Huang, C.; Li, X. First-in-Class Hydrazide-Based HDAC6 Selective Inhibitor with Potent Oral Anti-Inflammatory Activity by Attenuating NLRP3 Inflammasome Activation. *J. Med. Chem.* **2022**, *65* (18), 12140–12162. DOI: 10.1021/acs.jmedchem.2c00853. 08.09.2022.
- (17) Sinatra, L.; Yang, J.; Schliehe-Diecks, J.; Dienstbier, N.; Vogt, M.; Gebing, P.; Bachmann, L. M.; Sönnichsen, M.; Lenz, T.; Stühler, K.; Schöler, A.; Borkhardt, A.; Bhatia, S.; Hansen, F. K. Solid-Phase Synthesis of Cereblon-Recruiting Selective Histone Deacetylase 6 Degraders (HDAC6 PROTACs) with Antileukemic Activity. *J. Med. Chem.* **2022**, *65* (24), 16860–16878. DOI: 10.1021/acs.jmedchem.2c01659. 06.12.2022.
- (18) Hai, Y.; Christianson, D. W. Histone deacetylase 6 structure and molecular basis of catalysis and inhibition. *Nat. Chem. Biol.* **2016**, *12* (9), 741–747. DOI: 10.1038/nchembio.2134. 25.07.2016.
- (19) Bonandi, E.; Christodoulou, M. S.; Fumagalli, G.; Perdicchia, D.; Rastelli, G.; Passarella, D. The 1,2,3-triazole ring as a bioisostere in medicinal chemistry. *Drug Discov. Today* **2017**, *22* (10), 1572–1581. DOI: 10.1016/j.drudis.2017.05.014. 01.07.2017.
- (20) Galdeano, C.; Gadd, M. S.; Soares, P.; Scaffidi, S.; van Molle, I.; Birced, I.; Hewitt, S.; Dias, D. M.; Ciulli, A. Structure-guided design and optimization of small molecules targeting the protein-protein interaction between the von Hippel-Lindau (VHL) E3 ubiquitin ligase and the hypoxia inducible factor (HIF) alpha subunit with in vitro nanomolar affinities. *J. Med. Chem.* **2014**, *57* (20), 8657–8663. DOI: 10.1021/jm5011258. 06.10.2014.
- (21) Jin, J.; Yang, X.; Liu, J.; Xiong, Y.; Poulikakos, P.; Karoulia, Z.; Wu, X.; Ahmed, T. COMPOSITIONS AND METHODS FOR TREATING CDK4/6-MEDIATED CANCER. WO2017US65027 20171207.
- (22) Médard, G.; Sheltzer, J. M. Ricolinostat is not a highly selective HDAC6 inhibitor. *Nat. Cancer* **2023**, *4* (6), 807–808. DOI: 10.1038/s43018-023-00582-3.
- (23) Meier, F.; Brunner, A.-D.; Frank, M.; Ha, A.; Bludau, I.; Voytik, E.; Kaspar-Schoenefeld, S.; Lubeck, M.; Raether, O.; Bache, N.; Aebersold, R.; Collins, B. C.; Röst, H. L.; Mann, M. diaPASEF: parallel accumulation-serial fragmentation combined with data-independent acquisition. *Nat. Methods* **2020**, *17* (12), 1229–1236. DOI: 10.1038/s41592-020-00998-0. 30.11.2020.
- (24) Krönke, J.; Udeshi, N. D.; Narla, A.; Grauman, P.; Hurst, S. N.; McConkey, M.; Svinkina, T.; Heckl, D.; Comer, E.; Li, X.; Ciarlo, C.; Hartman, E.; Munshi, N.; Schenone, M.; Schreiber, S. L.; Carr, S. A.; Ebert, B. L. Lenalidomide causes selective degradation of IKZF1 and IKZF3 in multiple myeloma cells. *Science* **2014**, *343* (6168), 301–305. DOI: 10.1126/science.1244851. 29.11.2013.
- (25) Wang, S.; Fairall, L.; Pham, T. K.; Ragan, T. J.; Vashi, D.; Collins, M. O.; Dominguez, C.; Schwabe, J. W. R. A potential histone-chaperone activity for the MIER1 histone deacetylase complex. *Nucleic Acids Res.* **2023**, *51* (12), 6006–6019. DOI: 10.1093/nar/gkad294.
- (26) Xiong, Y.; Donovan, K. A.; Eleuteri, N. A.; Kirmani, N.; Yue, H.; Razov, A.; Krupnick, N. M.; Nowak, R. P.; Fischer, E. S. Chemo-proteomics exploration of HDAC degradability by small molecule degraders. *Cell Chem. Biol.* **2021**, *28* (10), 1514–1527.e4. DOI: 10.1016/j.chembiol.2021.07.002. 26.07.2021.
- (27) Yang, K.; Song, Y.; Xie, H.; Wu, H.; Wu, Y.-T.; Leisten, E. D.; Tang, W. Development of the first small molecule histone deacetylase 6 (HDAC6) degraders. *Bioorg. Med. Chem. Lett.* **2018**, *28* (14), 2493–2497. DOI: 10.1016/j.bmcl.2018.05.057. 30.05.2018.